OCCURRENCE OF LATE-EXPANSIVE ASR IN A GRANITOID ROCK WITH MICROGRAPHIC TEXTURE, HOKURIKU REGION, JAPAN

SATO Tomomi[1]*, HIRONO Shinichi[1], KUBO Yoshinori[2]

1 Taiheiyo Consultant Co., Ltd., Sakura, JAPAN

2 Kanazawa University, Kanazawa, JAPAN

Abstract

This paper reports an example of concrete deterioration due to late-expansive alkali-silica reaction (ASR) in a 45-year old bridge over Lake Kuzuryu, Fukui Prefecture, Hokuriku region, Japan. Core samples taken from reinforced concrete slabs were investigated petrographically. ASR occurred in granitoid rock with a micrographic texture containing microcrystalline quartz. In Japan, the only occurrence of ASR in granitoid rock rather than from a deformed rock containing cryptocrystalline quartz is from a cataclasite. However, ASR in granitoid rock free of secondary deformation was identified in this study. The graphic texture is a regular intergrowth of quartz and feldspar characteristic of these rocks. As the specific surface area of the quartz in this granitoid rock is large, similar to micro- to cryptocrystalline quartz in other slow-reactive rock types, the micrographic texture containing this quartz is believed to be capable of producing late-expansive ASR in concrete.

Keywords: alkali-silica reaction, petrographic examination, graphic texture, granitoid rock, microcrystalline quartz.

1. INTRODUCTION

Alkali-silica reaction (ASR) in granitoid rocks has been reported from continental regions of the world, eg. India [1], Brazil [2], Canada [3,4], Austrakia [5], Norway [6], Portugal [7], Thailand [8], and rarely in Japan [9]. All these reports primarily addressed granitic mylonite, granitic cataclasite, and other mechanically deformed rocks. Mylonite is formed when a faulted rock is subjected to plastic flow at depth. The structure of the host rock is generally polycrystallised and fine-grained. Cataclasite, a type of crushed rock that is solidified without recrystallization, forms when applied stress causes brittle fractures under relatively low temperature and pressure conditions in the shallow crust. Because granitoid rocks contain quartz, deformed areas of these rocks produce crypto- to microcrystalline quartz, which suggests that deformed granitoid rocks would show late expansive alkali-silica reactivity.

As previously stated, instances of ASR in the granitoid rocks free of mechanical deformation and associated cryptocrystalline quartz are extremely rare[10]. There is a report ASR possibly caused by opal in granitoid rock [11]. This study presents a case of ASR in the micrographic texture of granitoid rock extracted from a 45-year old bridge in the Hokuriku region of Japan. Graphic texture refers to the regularly patterned intergrowth texture unique to feldspar (alkali feldspar) and quartz, formed by simultaneous crystallization of the two minerals, micrographic texture refers to microscopic-sized graphic textures.

In this study, polarizing microscope, scanning electron microscope (SEM) and energy-dispersive x-ray spectroscopy (EDS) analysis on polished thin sections were used to elucidate details of the rock textures and
the occurrence of ASR.

2. GEOGRAPHICAL SETTING OF THE BRIDGE

Lake Kuzuryu is an artificial dam lake situated in the mountains (altitude 500 m) of Fukui Prefecture in Hokuriku region, Japan (Figure 1). The region of Lake Kuzuryu is rainy and snowy, annual precipitation between 2,100–3,400 mm and maximum snowfall of 1.0–2.5 m, temperature range from 35°C to -10°C [12].

The bridge studied here is situated over Lake Kuzuryu at Route 158 (Figure 1B, arrow). Constructed in 1967 at an elevation of about 570 m this bridge is a 64.7 m long steel plate girder bridge (Figure 2A).

* Correspondence to: Tomomi_Sato@taiheiyo-c.co.jp

The floor slabs were replaced in 2012, and slab samples were collected for analysis (Figure 2B). According to Ito et al. [13], removal of asphalt pavement revealed that in many parts of the upper surface of the floor slab, the concrete had been fragmented and rebar was exposed, showing severe deterioration. The lower surfaces of the floor slab had been previously reinforced by steel plate bonding (Figure 2C); however, the steel plates were no longer tightly bonded to the floor slabs. Water had accumulated in the resulting spaces, which likely accelerated freezing and thawing and ASR, resulting in considerable horizontal cracking (Figures 2B,D). Moreover, the traffic load on the bridge accelerated widening of the cracks [13]. Daily traffic volume of large vehicles on this bridge was about 600 in both directions.

3. MATERIAL AND METHODS

3.1 Optical microscope observation

For analysis, a concrete core sample, 8 cm in diameter × 19 cm in length (Figure 3A), was taken from the floor slab in the less deteriorated portion of the bridge. First, the sample was sliced into several sections in a longitudinal direction, and rock types and shapes of aggregates, and ASR-related changes in concrete were identified by stereomicroscopy. Modal analysis of coarse aggregates (short diameter > 5 mm) were made by counting the area ratio, by point-counting, in the cross-section.

Polished thin section (2 cm × 3 cm, 15–20 μm thick) containing ASR-reacted aggregate, were prepared for polarizing microscopy to reveal aggregate rock types, the occurrence of ASR, the structure of ASR gels, and the degree of cracking and other such deformation [14,15].

3.2 SEM observation and EDS analysis

Particles of granitoid rock were subjected to SEM observation (JEOL JSM-7001F) to confirm the occurrence of ASR, e.g., cracking in the aggregate and in the cement paste. Carbon coating was used on the surface of the polished thin sections. Back-scattered electron images (BEI) were used for image observation.

Polished thin sections previously observed by polarizing microscopy and SEM were used for quantitative analysis of ASR gels and other products, the surrounding crystals, and features representative of ASR gel generation in the granitoid. Quantification of the major elements (SiO_2, TiO_2, Al_2O_3, Fe_2O_3, MnO, MgO, CaO, Na_2O, K_2O, SO_3, P_2O_5) was performed by using EDS (Oxford INCA Penta FET x3) built into the SEM equipment. The measurement conditions were: acceleration voltage 15 kV, beam current 0.3 nA, measurement time 60s, and dead time 25%, using XPP correction. The analytical results are reported as raw values without normalization of the total value to 100%.

4. RESULTS

4.1 Optical microscope observation

Coarse aggregate was rounded gravel composed of many rock types (Figures 3A-C). The maximum size of the aggregate in core samples was about 40 mm (short axis). Fine aggregate was sand of various rock types common to the coarse aggregate, along with fragments of quartz and feldspar. Two types of cracks were present: one originating at the interior coarse aggregate particles (Figures 3B-G white arrows), while the other was horizontal cracks passing through the aggregate, fully penetrating the core sample (Figures 3A,B black arrows).

Occurrence of ASR was confirmed in rhyolitic welded ruff, rhyolite and granophyre particles in coarse aggregate (Figures 3B,D,E white arrows, Figures 4A-D), as well as in rhyolitic welded tuff, rhyolite (Figures 4G,H) and andesite in fine aggregate. Table 1 shows the progress of the reaction. Identified reactive minerals in rhyolitic welded tuff and rhyolite were cryptocrystalline quartz and glass, and in andesite were glass and cristobalite. In granophyre, typical reactive minerals, except for microcrystalline quartz, were not confirmed, but a micrographic texture was observed (Figures 4E,F).

The cement paste contained no fly ash or blast furnace slag powder, which means normal Portland cement was used. Further, this concrete had no air-entrained (AE) bubbles, and its durability against freeze/thaw was assumed to be low.

4.2 SEM observation and EDS analysis

The reactive phase of granophyre was confirmed through polarizing microscopy (Figures 4A-D, Table 1), and SEM observations performed for approximately the same position (Figures 5A-E). The photographs in Figures 5G and H show particles with a distinct micrographic texture. Parts along expansion cracks are filled with ASR gel that runs from inside the aggregate particles to the cement paste; micrographic texture was confirmed to be in contact with this gel (Figure 5B). At the boundary of regularly patterned intergrowth structures, feldspar (alkali feldspar) and quartz—light grey for feldspar and grey for quartz in BEI—, a substance with darker colour surrounding or intergranular to microcrystalline quartz crystals was present (Figures 5C,D). The EDS analysis revealed that this portion differs from the surrounding feldspar and quartz and is composed mainly of silica and minor amounts of sodium, potassium, aluminum, and calcium (Table 2). Furthermore, compared to quartz and feldspar, the total amount was low.

5. DISCUSSION

Micrographic textures are generally composed of holocrystalline, regular intergrowths in which crystals of quartz and feldspar are interwoven without gaps. However, in ASR affected concrete, Figures 5C and D show a structure with separated crystals surrounded by dark material. This is assumed to be a result of dissolution of quartz and/or feldspar, and formation of gel-like materials. Their composition differs from typical mica and allophane, suggesting that the substance in the gaps is ASR gel generated from the dissolution of the quartz. In addition, the amounts of calcium and alkalis (sodium and potassium) are less in this region than that in the nearby ASR gel (Table 2), which indicates a close proximity to the generation site. This is similar to the example from Newfoundland [16]. According to Katayama, when freeze-thaw cycles were superimposed, cracks and ASR gel developed due to migration of interstitial water during the cycles; a result of enhanced leaching of alkalis from ASR gel [16]. Based on there observations, the quartz constituting the micrographic texture is believed to have generated the ASR. If a graphic structure is sufficiently fine, then the constituent quartz is also fine, just as ordinary microcrystalline quartz, and its surface area is large.

Since the bridge where the samples were taken is located in a region of heavy snow, anti-freezing agents are sprayed on the bridge during winter. In addition, based on polarizing microscopy, entrained air voids were absent, thus durability against frost damage was assumed to be low. Therefore, it is possible that corrosion of cement paste by anti-freezing agents penetrating cracks occurring near the concrete surface and the concurrent of freeze/thaw damage promoted the ASR.

6. CONCLUSIONS

- Reported cases of ASR in granitoid aggregate are associated either with microcrystalline quartz in deformed rocks such as mylonite and cataclasite, or with secondary opal generated by alterations.
- The present study revealed an example of ASR in a granophyre (granitoid) with a micrographic texture that was not subjected to mechanical deformation or metamorphosis.
- Because the graphic texture examined here was sufficiently fine (micrographic texture), microcrystalline quartz, the quartz in this micrographic texture having an increased surface area in this rock should be regarded as a reactive mineral.

ACKNOWLEDGEMENTS

We are grateful to the Road Maintenance Division in the Okuetsu Civil Engineering Office of Fukui Prefecture for providing samples for analysis. We are also grateful to Dr. Katayama of Taiheiyo Consultant Co., for his advice.

7. REFERENCES

[1] Gogte, BS (1973): An evaluation of some common Indian rocks with special reference to alkali-aggregate reactions. Engineering Geology (7): 135-153.

[2] Cavalcanti, AJCT (1987): Alkali-aggregate reaction at Moxoto Dam, Brazil. Proceedings of 7th ICAAR, Ottawa: 168-172.

[3] Grattan-Bellew, PE (1987): Is high undulatory extinction in quartz indicative of alkali-expansivity of granitic aggregates? Proceedings of the 7th ICAAR, Ottawa: 434-439.

[4] Grattan-Bellew, PE (1990): Canadian experience with the mortar bar accelerated test for alkali-aggregate reactivity. In: Canadian developments in testing concrete aggregates for alkali–aggregate reactivity. Engineering Materials Office, Ministry of Transportation, Downsview, Ontario: Report EM-92: 17–34.

[5] Shayan, A (1993): Alkali-reactivity of deformed granitic rocks: a case study. Cement and Concrete Research (23):1229-1236.

[6] Wigum, BJ (1995): Examination of microstructural features of Norwegian cataclastic rocks and their use for predicting alkali-reactivity in concrete. Engineering Geology (40): 195-214.

[7] Fernandes, I, Noronha, F, Teles, M (2007): Examination of the concrete from an old Portuguese dam. Texture and composition of alkali-silica gel, Materials Characterization (58): 1160-1170.

[8] Hirono, S, Yamada, K, Ando, Y, and Torii, K (2015): ASR Problems in Japan and a Case of ASR Found in Thailand. Proceedings of the 14th ICCC, Beijing China: CD-R (5), 10p.

[9] Nomura, M, Hirono, S, and Daidai, T (2014): Alkali-Silica Reaction in granitoid rock, in Toyama prefecture. Proceedings of the 69th JSCE Annual Meeting: 969-970. (in Japanese)

[10] Fernandes, I (2015): Role of granitic aggregates in the deterioration of a concrete dam. Bulletin of Engineering Geology and the Environment. (74): 195-206.

[11] Thaulow, N (1983): Alkali-Silica Reaction in the Itezhitezhi Dam Project, Zambia. Proceedings of the 6th ICAAR, Copenhagen: 471-477.

[12] Japan Meteorological Aency HP: 2004-2014, On http://www.jma.go.jp/jma/menu/menureport.html

[13] Ito, Y, Shimada, M, Goto, T, Shibata, T and Ota, K, (2013): Investigation On Road-bridge Slab affected by Alkali-Silica Reactions, Civil Engineering Journal 55(8): 56-59. (in Japanese)

[14] Katayama, T, Oshiro, T, Sarai, Y, Zaha, K, and Yamato, T (2008): Late-Expansive ASR due to Imported Sand and Local Aggregates in Okinawa Island, Southwestern Japan. Proceedings of the 13th ICAAR, Trondheim : 862-873.

[15] Katayama, T (2012): Late-expansive ASR in a 30-year old PC structure in Eastern Japan. Proceedings, 14th ICAAR, Austin (paper 030411-KATA-05): 10p.

[16] Katayama, T (2008): ASR gel in concrete subject to freeze-thaw cycles - Comparison between laboratory and field concretes from Newfoundland, Canada. Proceedings of the 13th ICAAR, Trondheim: 174-183.

TABLE 1: Intensity and stage of ASR with reference to the reacted rock types of the aggregate in concrete as determined by thin section petrography. (based on [11,12])

Rock types		Progress of ASR →					Petrographic severity of ASR
		In aggregate	In cement paste	In aggregate	In cement paste		
		Reaction rim	Sol/gel exudation	Gel-filled cracks		Gel-filled void distinct from aggregate	
Coarse aggregate	Rryholitic welded tuff and rhyolite †	○	○	○	○	+	2-3
	Granophyre †	○	○	○	○		2
Fine aggregate	Rryholitic welded tuff and rhyolite †	○	○	+			1-2
	Andesite ‡	○	○				1

Intensity of ASR: ● conspicuous, ○ present, + trace
Petrographic severity of ASR: 1 traceable (cryptic stage) , 2 moderate (developing stage / accelerating stage), 3 severe (accelerating stage /deteriorating stage)
Type of reaction: † late-expansive, ‡ early-expansive

TABLE 2: Selected compositions of ASR gel, and minerals in granophyre in concreate as determined by EDS analysis on polished thin section.

	ASR gel					Granophyre	
	In cement paste	In rock (outer)	In rock (inner)	Intergranular (ASR gel fomed on quartz)		microcrystalline	
						Quartz	Feldspar
Number #	1	2	3	4	5	6	7
SiO_2	51.51	56.88	56.44	79.55	76.54	99.02	64.93
TiO_2	0.03	0.10	0.00	0.22	0.02	0.02	0.00
Al_2O_3	0.33	0.75	0.81	1.26	1.25	0.42	16.74
Fe_2O_3	0.07	0.08	0.14	0.17	0.10	0.00	0.00
MnO	0.00	0.10	0.00	0.00	0.00	0.12	0.00
MgO	0.00	0.10	0.03	0.00	0.01	0.00	0.11
CaO	24.13	22.01	18.15	3.58	7.03	0.10	0.25
Na_2O	0.04	0.52	0.43	0.08	0.06	0.00	0.25
K_2O	0.59	2.47	2.02	0.95	0.75	0.04	16.37
SO_3	0.00	0.06	0.05	0.00	0.19	0.08	0.06
P_2O_5	0.00	0.00	0.00	0.00	0.00	0.07	0.05
Total	76.71	83.07	78.05	85.82	85.96	99.87	98.74
[Ca/Si]*	0.50	0.41	0.34	0.05	0.10		
[Ca]/ [Na+K]*	30.98	5.70	5.73	2.81	7.14		

#: Analysis point numbers (see Figure 5).
*: Atomic ratio.

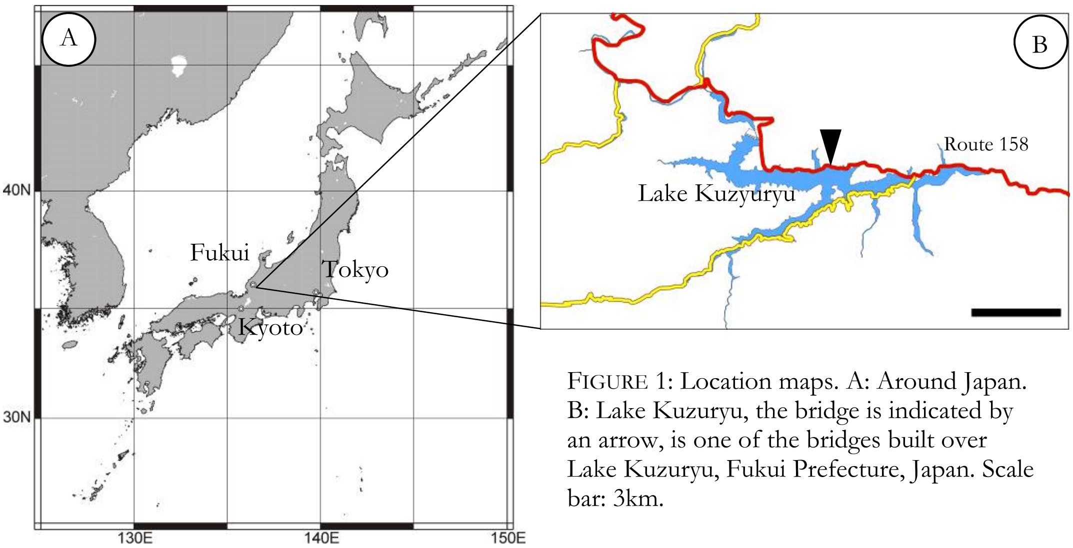

FIGURE 1: Location maps. A: Around Japan. B: Lake Kuzuryu, the bridge is indicated by an arrow, is one of the bridges built over Lake Kuzuryu, Fukui Prefecture, Japan. Scale bar: 3km.

FIGURE 2: Site of the bridge. A: Overview. B: Borehole in the concrete slab after removal of asphalt layer. C: View from under the bridge. D: ASR-deteriorated structure.

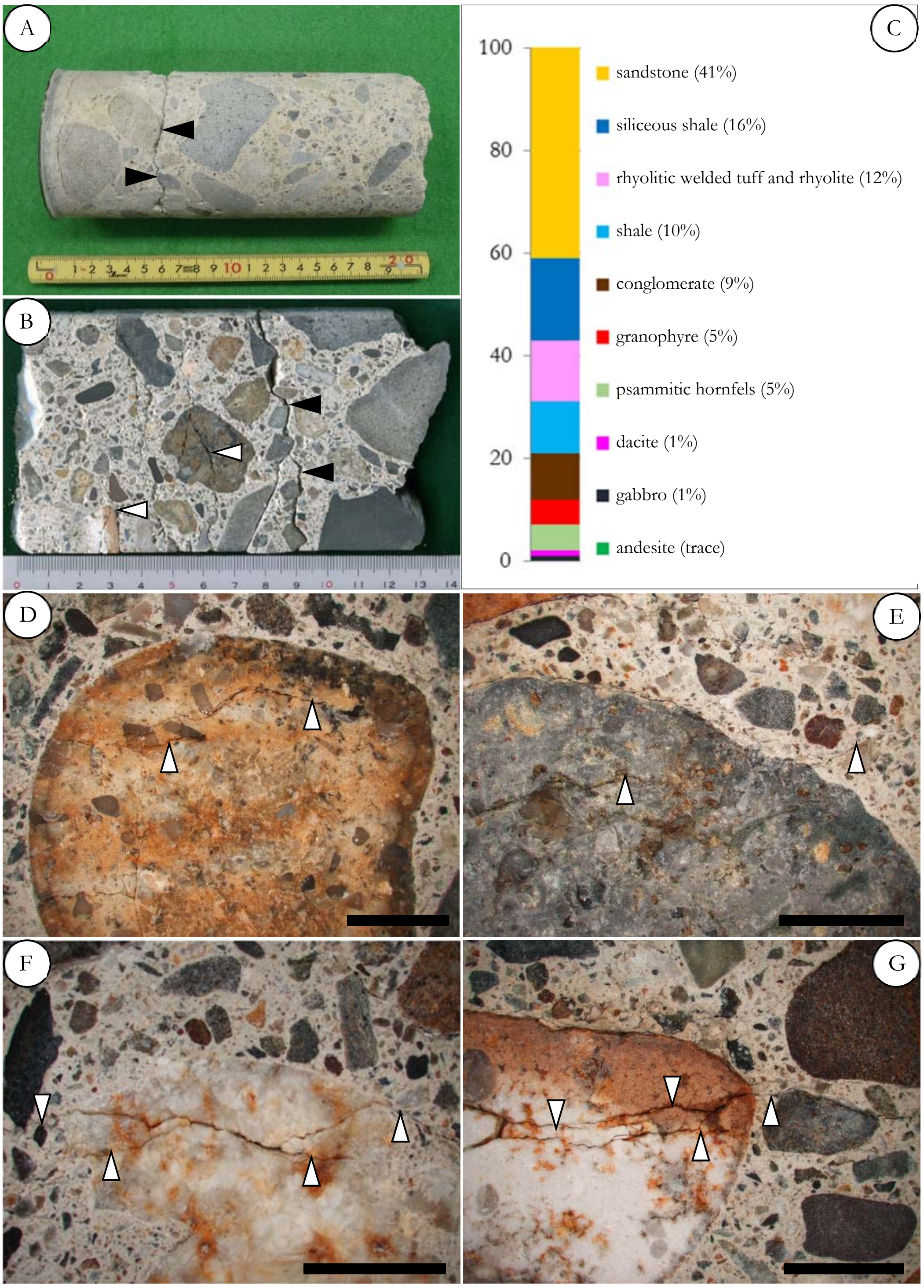

FIGURE 3: Microscopic features of concrete and coarse aggregate. A: Slab concrete core sample, left side is surface. B: Sliced section, scanned image. C: Rock types of coarse aggregate (vol%). D,E: Rhyolitic welded tuff, coarse aggregate. F,G: Granophyre, coarse aggregate. Black and white arrows point to cracks, white arrows originate from ASR. Scale bar: D-G 5mm.

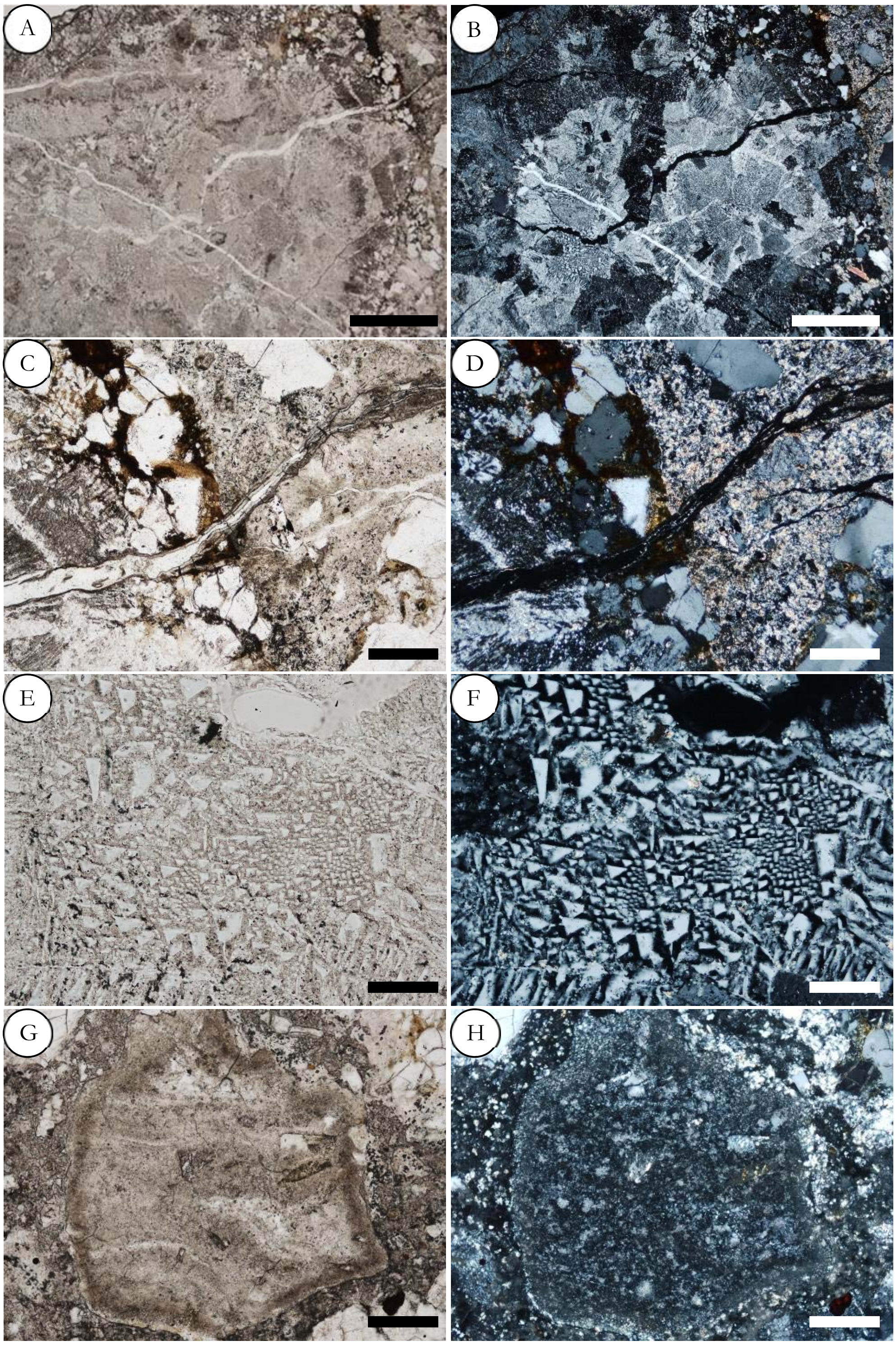

FIGURE 4: Photographs of polarizing microscopy. A-F: Granophyre of the coarse aggregate, left side are lower polar and right side are crossed-polar images. C,D: ASR gel-filled cracks in aggregate and cement paste. E,F: Typical formation of the micrographic texture. G,H: Reaction rim, rhyolitic welded tuff, holohyaline, fine aggregate. Scale bar: A,B 1mm, C,D 0.2mm, E-H 0.1mm.

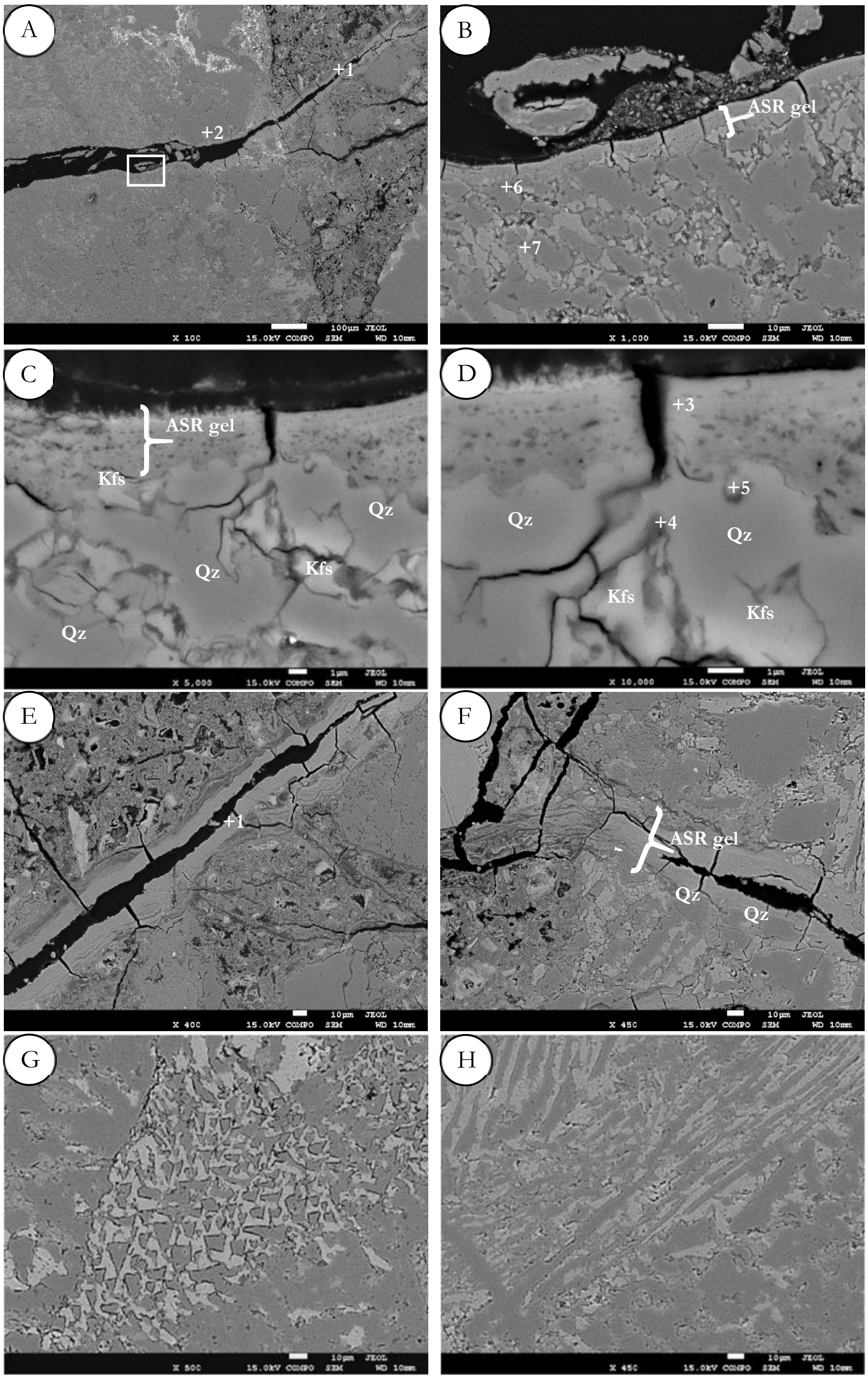

FIGURE 5: SEM images (BEI) on polished thin sections. A-H: Granophyre of the coarse aggregate. A: ASR gel-filled cracks extending from aggregate into cement paste. B-D: Field of ASR, enlargements inside the frame of A. D: Intergranular ASR gel formed on microcrystalline quartz. E: ASR gel-filled cracks in cement paste. F: ASR gel-filled cracks in aggregate. G,H: Typical micrographic texture. Gray is quartz (Qz), light gray is feldspar (Kfs). Numbers are EDS analysis point (see Table 2). Scale bar: A 100μm, B,E-H 10μm, C,D 1μm.